Leif-Erik Bohman, MD

Department of Neurological Surgery,
Columbia University College of Physicians and Surgeons,
New York, New York

Kristin R. Swanson, PhD

Department of Pathology,
University of Washington,
Laboratory of Neuropathology,
Harborview Medical Center,
Seattle, Washington

Julia L. Moore, BS

Department of Pathology,
University of Washington,
Laboratory of Neuropathology,
Harborview Medical Center,
Seattle, Washington

Russ Rockne, MS

Department of Pathology,
University of Washington,
Laboratory of Neuropathology,
Harborview Medical Center,
Seattle, Washington

Christopher Mandigo, MD

Department of Neurological Surgery,
Columbia University College of Physicians and Surgeons,
New York, New York

Todd Hankinson, MD, MBA

Department of Neurological Surgery,
Columbia University College of Physicians and Surgeons,
New York, New York

Marcela Assanah, PhD

Division of Neuropathology,
Department of Pathology,
Columbia University Medical Center,
New York, New York

Peter Canoll, MD, PhD

Division of Neuropathology,
Department of Pathology,
Columbia University Medical Center,
New York, New York

Jeffrey N. Bruce, MD

Department of Neurological Surgery,
Columbia University College of Physicians and Surgeons,
New York, New York

Reprint requests:
Dr Leif-Erik Bohman, MD,
University of Pennsylvania Health Services,
Department of Neurosurgery,
3400 Spruce St,
3 Silverstein,
Philadelphia, PA 19104.

Received, October 18, 2009.
Accepted, May 7, 2010.

Magnetic Resonance Imaging Characteristics of Glioblastoma Multiforme: Implications for Understanding Glioma Ontogeny

BACKGROUND: Identifying the origin of gliomas carries important implications for advancing the treatment of these recalcitrant tumors. Recent research promotes the hypothesis of a subventricular zone (SVZ) origin for the stemlike gliomagenic cells identified within human glioma specimens. However, conflicting evidence suggests that SVZ-like cells are not uniquely gliomagenic but this capacity may be shared by cycling progenitors distributed throughout the subcortical white matter (SCWM).

OBJECTIVE: To review radiological evidence in glioblastoma multiforme (GBM) patients to provide insight into the question of glioma ontogeny.

METHODS: We explored whether GBMs at first diagnosis demonstrated a pattern of anatomic distribution consistent with origin at the SVZ through retrospective analysis of preoperative contrast-enhanced T1-weighted magnetic resonance images in 63 patients. We then examined the relationship of tumor volume, point of origin, and proximity to the ventricles using a computer model of glioma growth.

RESULTS: Fewer than half of the GBMs analyzed had contrast-enhancing portions that contacted the ventricle on preoperative imaging. A strong correlation was found between tumor volume and the distance between the contrast-enhancing edge of the tumor and the ventricle, demonstrating that tumors abutting the ventricle are significantly larger than those that do not. The lesions simulated by the computer model validated our assumption that tumors that are radiographically distant from the ventricles are unlikely to have originated in the SVZ and supported our hypothesis that as they grow, the edges of all tumors will near the ventricles, regardless of their point of origin.

CONCLUSION: This work offers further support for the hypothesis that the origins of GBMs are at sites distributed throughout the white matter and are not limited to the region of the SVZ.

KEY WORDS: Cancer stem cell, Glioblastoma, Glioma, Glioma ontogeny

Neurosurgery 67:1319–1328, 2010 DOI: 10.1227/NEU.0b013e3181f556ab www.neurosurgery-online.com

Glioblastoma multiforme (GBM), the most common malignant intracranial neoplasm in adults, carries a dismal prognosis. Gliomas can arise throughout the central nervous system but are always found in the subcortical white matter (SCWM). The notion of a "cancer stem cell" has gained increasing popularity, fueled by the recent discovery of cells with stemlike properties within human gliomas.[1-5] Although the concept of cancer stem cells and the notion that gliomas may arise from stem or stemlike cells in the central nervous system are distinct, many studies have focused on neural stem cells in the subventricular zone (SVZ) as the "cell of origin" for all gliomas.[6-8] There is growing evidence that glial progenitors that are abundant and widely distributed throughout the brain also have the

ABBREVIATIONS: **CPVD**, center point–to-ventricle distance; **EVD**, edge-to-ventricle distance; **GBM**, glioblastoma multiforme; **SCWM**, subcortical white matter; **SVZ**, subventricular zone

capacity to form gliomas.[9-15] However, recent articles still support the hypothesis that neural stem cells/progenitors in the SVZ are uniquely capable of forming glioblastomas,[16-18] some suggesting that even tumors distant from the SVZ may arise there[19,20] and that the SVZ should be therapeutically targeted in patients with GBM to prevent recurrence.[21] In view of these conflicting viewpoints, we reviewed radiological evidence in GBM patients to provide insight into this question of glioma ontogeny.

To understand the implications on glioma ontogeny in a study of GBMs on preoperative magnetic resonance imaging (MRI), 3 assumptions were made. The first assumption was that the cells that give rise to tumors are potentially distributed widely throughout the brain. The second assumption was that tumors begin as a point of origin and grow by radial dispersion into the surrounding brain tissue. The final assumption was that the patterns of dispersion would depend on the geometry of the tissue boundaries, including the gray white junctions and the pial and ventricular margins.

From these assumptions, 3 predictions were made regarding the patterns likely to be observed. First, tumors originating at points in the white matter distant from the SVZ might approach or abut the SVZ as they grow. Therefore, the distance from the ventricle to the nearest edge of the tumor would negatively correlate with tumor volume. Second, for tumors that arise in the white matter, the distances between the tumor center and the ventricle should not show a clear relationship to tumor volume because the center of the tumor should remain relatively static as the tumor grows radially. Third, in tumors that originate at the SVZ, the distance between the center of the tumor and the ventricle should increase as the tumor increases in size because, as the radial growth of the tumor is constrained by the ventricle in one direction, the center will be displaced away from the ventricle as the tumor grows.

Use of Computerized Simulations of Glioma Growth

We sought to further explore our assumptions and to test our hypotheses using computerized simulations of glioma growth and invasion. Based on serial imaging and algorithms that factor in tumor cell net proliferation rates and migration rates in gray and white matter, computerized models have been validated to accurately map glioma growth in MRI over time.[22] The model accurately predicts growth patterns of gliomas of all grades, both untreated[23–27] and treated.[28-31] Because it is impossible radiographically to know precisely where a human GBM arises, we used this validated model of glioma growth (where the point of origin is user determined) to test whether tumors displaying clinically observed patterns of growth could originate at the SVZ yet appear radiographically distant from the ventricles. Simulated tumor growth allowed us to investigate growth patterns and the spatial evolution and location of the contrast-enhancing center of mass relative to a known point of origin.

PATIENTS AND METHODS

Patient Selection

Columbia University Medical Center Department of Neuropathology records were searched to identify patients with histologically diagnosed World Health Organization grade IV astrocytomas (GBM) from 2004 to 2006. Among patients with newly diagnosed GBM, 84 consecutive preoperative patients with fine-cut contrast-enhanced preoperative MRIs performed at Columbia were reviewed. Patients were excluded for prior craniotomy (n = 10), absence of contrast-enhancing lesion (n = 2), multiple contrast-enhancing lesions (n = 5), and bilateral lesions (n = 4). A total of 21 patients were excluded, leaving a total of 63 patients included in the study. For 1 patient, we were able to obtain 2 preoperative scans separated by approximately 1 month (34 days). For the primary analysis, only the most recent fine-cut MRI study was used. The additional (1 month preoperatively) scan was not included in the primary analysis, but the patient's 2 scans were compared to help validate study assumptions about tumor growth patterns over time.

Data Collection and Analysis

All MRIs were collected as DICOM-format data and analyzed with OsiriX version 2.5.1 on an Apple Powerbook G4. Sagittal and coronal series were generated with the OsiriX "orthogonal reslice" tool to generate 256 slice reconstructions. All analyses were done by a single researcher (L.E.B.) to eliminate interobserver variability in technique. In each plane, the largest contrast-enhancing portion of the tumor was identified and measured along 2 axes. Tumor volume was estimated by using half of the average diameters of the tumor in each plane along each axis and treating the tumor as a sphere where $V = (4/3)\pi r^3$. A second method, measuring the area of a tracing around the enhancing portion of the tumor in each plane, was used for validation with minimal variability (data not shown).

The distance between the edge of the tumor and the ventricles (referred to as the edge-to-ventricle distance [EVD]) was measured as the shortest distance between the enhancing rim of the tumor and the edge of the ventricle in any slice in each plane. For each tumor, the minimum EVD observed (in any slice, in any plane) was used for analysis. The center of each tumor in each plane was estimated as the intersection between the greatest tumor dimension along 2 axes. The distance between the center point of the tumor and the ventricles (referred to as the center point–to-ventricle distance [CPVD]) was measured using 2 methods for each tumor. The first method was to measure the shortest distance between the estimated center point of the tumor and the edge of the ventricle in each plane. Because the estimated center point of the tumor and the shortest distance between the center point and the ventricle may not lie in the same slice in any given plane, the second method for determining the CPVD calculated, using the Pythagorean theorem, the hypotenuse of a triangle in which the 2 short sides of the triangle were the radius of the tumor and the EVD in that plane. The shortest observed or calculated CPVD from any plane was used for analysis.

Biomathematical Modeling and Simulation

Using the BrainWeb brain atlas[32] at 1-mm^3 resolution, we performed simulations of glioma growth with methods established by Swanson et al.[22,26,33] The rate of change in glioma cell concentration, c(x,t), over time can be expressed as the summation of net rates of migration and proliferation as follows:

$$\overbrace{\frac{\partial c}{\partial t}}^{\text{rate of change of glioma cell concentration}} = \overbrace{\nabla \cdot (D(x)\nabla c)}^{\text{net dispersal of glioma cells}} + \overbrace{\rho c\left(1-\frac{c}{K}\right)}^{\text{net proliferation of glioma cells}}$$

where ∇ represents the spatial gradient. D (mm^2/y) represents the net dispersal or migration rate of glioma cells in undifferentiated brain tissue; $D(x) = D_g$ is the dispersal rate associated with glioma cells at a location x in gray matter and $D(x) = D_w$ is another dispersal rate associated with glioma cells at a location x in white matter. The migration rate in white matter is generally thought to be larger than that in gray matter, $D_w > D_g$, [34] and may be affected by the fiber orientation in this tissue, making it possible for D to be a tensor D.[35] The parameter ρ (1/y) represents the net rate of increase in number of tumor cells, including proliferation and cell loss, and K represents the slowing of the net proliferation rate to accommodate the carrying capacity of the tissue, providing an upper limit on the number of cells capable of occupying any cubic millimeter of volume.

Virtual tumors were initiated with a concentration of 10^3 glioma cells within the 1-mm^3 voxel defined as the in silico origin. With the technique of Harpold et al,[22] in silico MRI abnormalities were defined as voxels with tumor cell concentration greater than previously estimated limits. The tumor center was computed as the center of mass of the simulated volume.

We chose tumor "start points" for the simulations on the basis of the existing literature regarding the SVZ and our own experience with glial progenitors in the SCWM. Coordinates for each start point in the BrainWeb online brain atlas are listed in Table 1. Of primary interest were areas within the SVZ that appeared, on the basis of the literature, to have high densities of cycling stemlike cells. The simulation start points were identified on McGill University's BrainWeb Atlas.[11] Using the descriptions and graphical representations of cycling cell density in the astrocytes ribbon of the SVZ by Sanai et al[36] and Quinones-Hinojosa et al,[8] we chose 3 points within the anterior SVZ: one in the ventral portion, one in the dorsolateral portion, and one intermediate between them. We also chose a point on the dorsolateral portion of the body of the SVZ, an intermediate point on the atrium of the SVZ, one on the lateral temporal portion of the ventricle, and one on the mesial portion of the ventricle, for a total of 5 SVZ start points overall.[8,36] We then selected 5 points in the white matter: one in the deep frontal white matter, one in the superficial frontal white matter, one in the white matter radial from the body of the SVZ, one in the superficial parietal white matter, and one in the deep temporal tip white matter.

Although there is a wide variation in the model parameters (D and ρ) across the glioblastoma population, we chose representative median values from our experience with glioblastoma patients.[22] This choice of a single set of parameter values allows direct comparison between the simulations because the relative time course of the in silico simulations should be similar and any differences seen can be interpreted as highlighting the effects of spatial variability associated with different start points. Locoregional differences in the gray/white distribution and the relative distance to boundaries (eg, ventricles or pia) will affect the time between the start of the simulation at 10^3 cells and the visible appearance of the "tip of the iceberg" of that lesion seen on clinical imaging.

RESULTS

Analysis of Preoperative MRIs

The general results are summarized in Table 2. Overall, fewer than half of the tumors abutted the ventricle. Of those that did not abut the ventricle, three-quarters were at least 5 mm away, and a fifth were > 10 mm from the nearest ventricle. Generally, the tumors were well distributed throughout the brain, with no clear predilection for any one lobe or hemisphere.

Tumor volume appeared closely related with the proximity of the tumors to the ventricles. Tumors that abutted the ventricle were significantly larger, with an average volume of 36.4 cm^3 compared with 23.7 cm^3 for tumors not abutting the ventricles ($P = .008$). When the tumors were analyzed in 2 groups divided by ventricular contact (see Figure 1), those tumors not abutting

TABLE 1. Brainweb Coordinates for Simulated Lesion Start Points[a]

Start Point Name	X	Y	Z
SVZ			
Anterior dorsolateral SVZ	18	16	18
Anterior intermediate SVZ	10	16	10
Anterior ventral SVZ	48	16	18
Body dorsolateral SVZ	18	−12	30
Atrium intermediate SVZ	32	−42	10
Temporal lateral SVZ	42	−8	−18
Mesial SVZ	34	-8	−20
SCWM			
Anterior superficial WM	48	16	18
Anterior deep WM	26	34	18
Body superficial WM	52	−26	30
Atrium superficial WM	52	−40	−8
Deep WM	48	−18	−18

[a]SCWM, subcortical white matter; SVZ, subventricular zone. The BrainWeb atlas was used to designate start points for the simulated brain tumors starting in the SVZ or SCWM based on anatomic descriptions found in the literature (see text). These are the coordinates used.

TABLE 2. General Results

Patients, n	63
Mean (median) tumor volume, cm^3	29.6 (22.0)
Right side, % (n)	46 (29)
Tumor locations (mutually exclusive), % (n)	
Frontal	33.3 (21)
Parietal	27.0 (17)
Temporal	34.9 (22)
Occipital	3.2 (2)
Basal ganglia	1.6 (1)
Mean (median) center point-ventricle distance, cm	2.9 (2.8)
Mean (median) edge-ventricle distance, mm	5.6 (2.9)
Distribution of tumors relative to ventricles, % (n)	
Abutting ventricles	46.0 (29)
Edge 0-2.5 mm from ventricle	1.6 (1)
Edge 2.5-5 mm from ventricle	11.1 (7)
Edge 5-7.5 mm from ventricle	9.5 (6)
Edge 7.5-10 mm from ventricle	11.1 (7)
Edge > 10 mm from ventricle	20.6 (13)

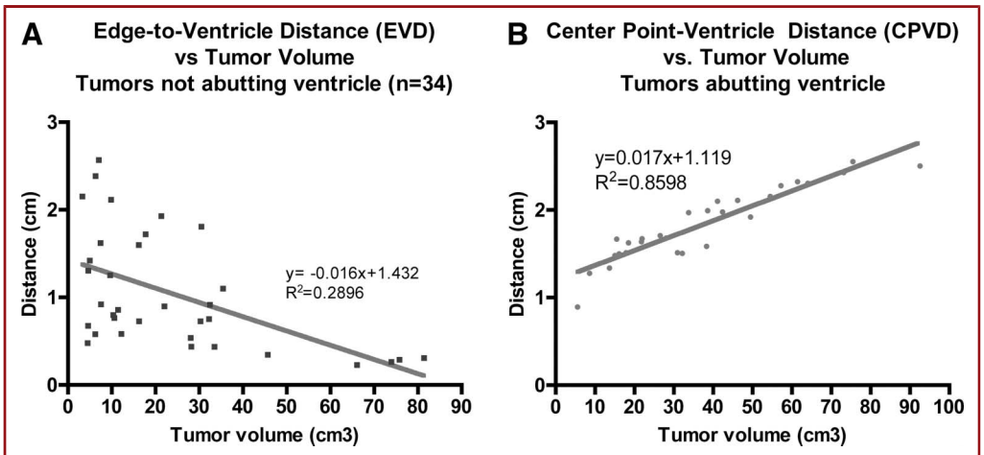

FIGURE 1. **A**, *edge-to-ventricle distance (EVD) plotted against tumor volume for tumors not abutting the ventricle; the best-fit line is shown. Tumor volume and EVD showed significant negative correlation (Spearman r = -0.53, P = .001).* **B**, *center point–to-ventricle distance (CPVD) plotted against tumor volume for tumors abutting the ventricle; the best-fit line is shown. Tumor volume and CPVD showed significant positive correlation (Spearman r = 0.93, P < .001). The same analysis performed on tumors not abutting the ventricle showed no significant correlation between CPVD and tumor volume (Spearman r = 0.18, P = .31).*

the ventricle showed a significant negative correlation between the EVD and tumor volume (Spearman $r = -0.5294$, $P = .001$) but no significant correlation between the tumor CPVD and tumor volume (Spearman $r = 0.1798$, $P = .31$). On the other hand, tumors abutting the ventricles showed a very strong relationship between the tumor CPVD and tumor volume (Spearman $r = 0.93$, $P < .001$).

The only significant differences found in analyzing data by lobe were that tumors in the temporal lobe tended to be smaller and were more likely to abut the ventricle than tumors in other lobes (Table 3). This difference is unsurprising given the anatomic differences among the lobes.

Illustrative Example: Serial Preoperative Images for 1 Patient

Although serial preoperative imaging was rarely performed, 1 patient who presented with a small mass was followed up radiographically over a 1-month period. During that interval, the tumor grew considerably, from a small mass distant from the ventricles to a moderately sized mass closer to the ventricles. Example images from those studies are included in Figure 2, along with the estimated tumor volume, EVD, and CPVD for each time point. Over the 1-month period, the tumor volume expanded 19-fold. With increasing volume, the EVD decreased markedly while the CPVD remained virtually unchanged. This is consistent with our predicted growth pattern for tumors growing distant from the SVZ.

Glioma Growth Model Simulations

Example screenshots for three of the simulated lesions are provided in Figure 3. Table 4 summarizes the simulation results, including the time from initiation of the simulation to the model-predicted appearance on T1-weighted, gadolinium-enhanced MRI. The table includes details of the relative distance of the origins from the nearest point on the ventricle and skull. These distances are compared with the time and volume at simulated contact between the contrast-enhancing volume and the ventricle and skull.

Tumors originating at points distant to the SVZ (n = 5 simulations) appeared on imaging to be distant from the SVZ as well, although as the tumors grew, they invariably neared and eventually contacted the SVZ, often at relatively modest tumor volumes (mean, 20.0 cm^3; range, 3.1-40.3 cm^3). Tumors of SVZ origin (n = 7 simulations) grew near or in contact with the SVZ at all time points, with at most brief intervals (< 30 days) of appearance on T1 at short distances from the ventricles. Simulated tumors starting at the SVZ showed increasing distance between the tumor center and ventricle over time (with increasing tumor size). Simulated tumors starting in the white matter, on the other hand, showed decreases in the distance between the ventricle and both the tumor edge and center over time (see Figure 4). These

TABLE 3. Differences in Volume, Edge-Ventricle Distance, and Center Point–Ventricle Distance by Brain Region[a]

	Frontal	Parietal	Temporal	*P* (by ANOVA)
Tumors, n	21	17	22	. . .
Mean tumor volume, cm^3	33.18	20.54	34.51	.13
Mean EVD, mm	0.7179	0.8202	0.296	.05
Mean CPVD, cm	2.422	2.253	2.124	.46
Abutting ventricle, %	33.3	23.5	68.2	.01

[a]ANOVA, analysis of variance; cPVD, center point–ventricle distance; EVD, edge-ventricle distance.

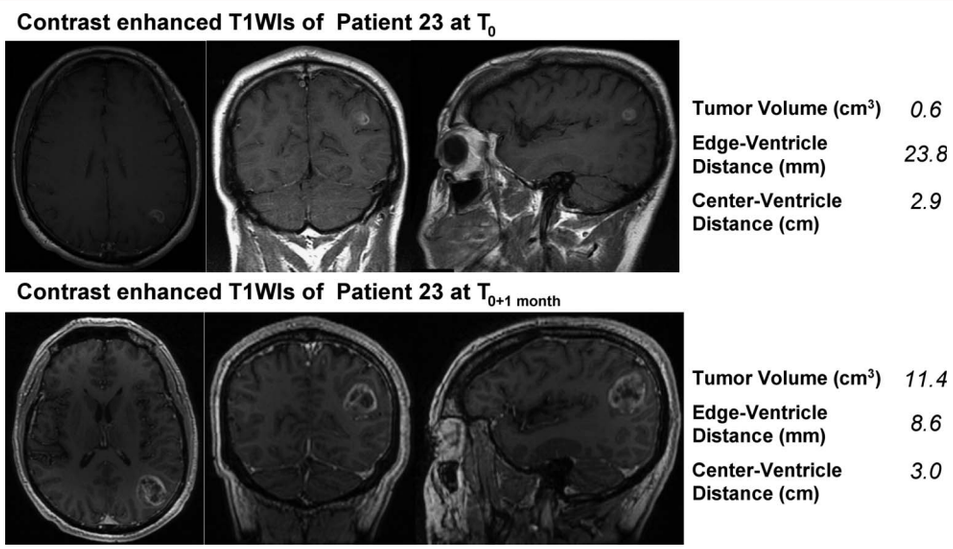

FIGURE 2. *Results of serial imaging for study patient 23.*

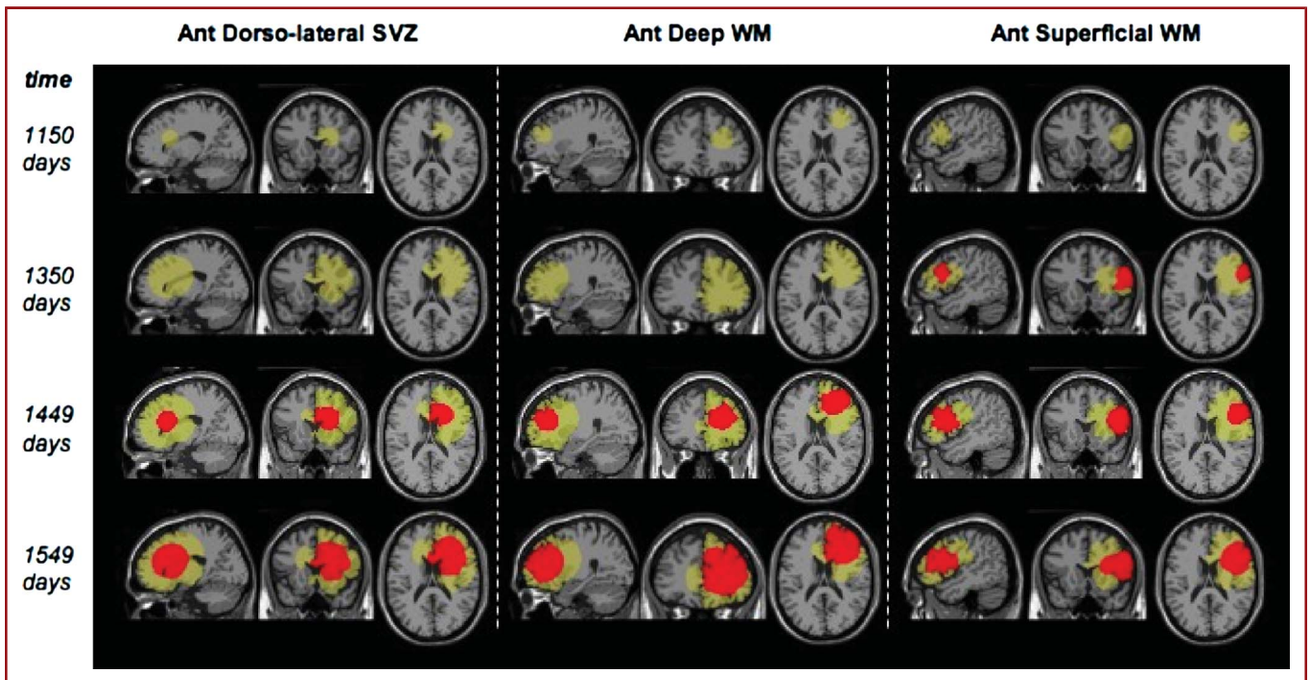

FIGURE 3. *Example screenshots from glioma growth model simulations with varied points of origin. Images at 4 time points each for 3 simulated lesions provided in the sagittal, coronal, and axial planes for lesion start points at the anterior dorsolateral subventricular zone, anterior deep white matter, and anterior superficial white matter. Green area reflects estimated T2-weighted image abnormality on magnetic resonance; red area reflects estimated T1-weighted image postgadolinium abnormality.*

TABLE 4. Simulated Lesion Results[a]

Start Point Name	Time Until Detectable on T1Gd, d	Distance From Origin to Ventricle, mm	Time from Detectable Until Edge-Ventricle Contact, d	T1Gd Volume at Edge-Ventricle Contact, cm^3	Distance From Origin to Skull, mm	Time From Detectable Until Edge-Skull Contact, d	T1Gd Volume at Edge-Skull Contact, cm^3	Time to Edge-Ventricle and Edge-Skull Contact, d	Volume to Edge-Ventricle and Edge-Skull Contact, cm^3
SVZ									
Anterior dorsolateral	1311	2	0	0.0	40	341	196.4	341	196.4
Body dorsolateral	1362	1	19	0.6	44	250	164.5	250	164.5
Anterior ventral	1009	1	0	0.0	27	626	46.9	626	46.9
Atrium interior	1357	1	3	0.0	37	224	127.1	224	127.1
Temporal lateral	1289	4	29	0.1	22	111	14.8	111	14.8
Anterior intermediate	977	1	0	0.0	35	846	151.2	846	151.2
Mesial	970	1	0	0.0	19	567	26.8	567	26.8
SCWM									
Anterior deep	1361	14	50	10.3	25	91	33.7	91	33.7
Body superficial	1255	30	241	34.6	18	42	1.2	241	34.6
Anterior superficial	1284	30	246	40.3	18	31	2.6	246	40.3
Atrium superficial	1308	15	77	11.5	20	38	2.9	77	11.5
Deep	1286	9	65	3.1	14	20	0.1	65	3.1

[a]SCWM, subcortical white matter; SVZ, subventricular zone; T1Gd, T1-weighted gadolinium.

patterns over time in the simulated tumors paralleled those observed in patient MRIs correlating CPVD and EVD to tumor volume.

To assess whether the center of the imaging abnormality reasonably estimates the point of origin, Figure 5 shows the distance from the origin to the center of mass of the simulated glioma over time for both SVZ (a) and SCWM (b) origins. The origin was generally within 1.25 cm of the center of mass but with significant variation with tumor size and location.

Because of the assertions by Lim et al[37] regarding tumors that invade both the cortex and SVZ, we were interested in whether there was a difference in the speed at which tumors starting in the SCWM or SVZ contacted both the skull (as a proxy for cortex) and the ventricle. Despite our small number of simulations, we found that simulated lesions starting in the SCWM achieved simultaneous ventricular and skull contact significantly more rapidly than those starting at the SVZ (mean time, 100 days for SCWM start points versus 420 days for SVZ start points;

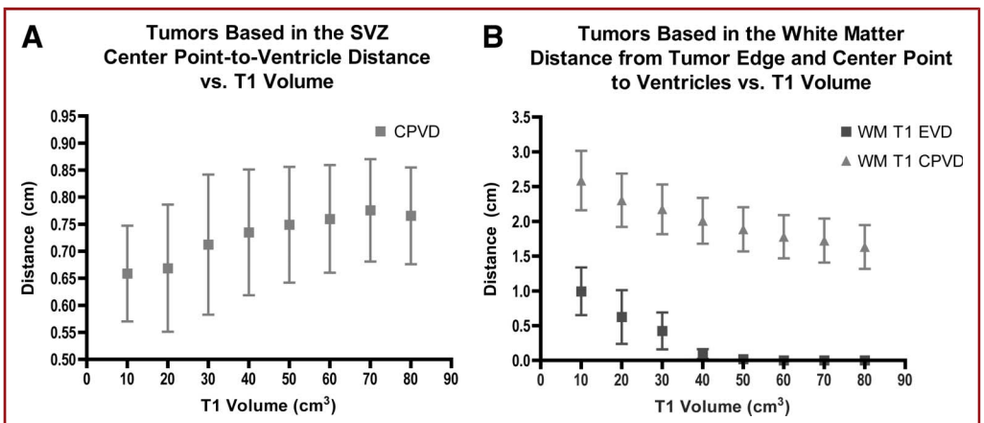

FIGURE 4. **A**, *center point–to-ventricle distance (CPVD) plotted against T1-weighted, gadolinium-enhanced (T1Gd) volume for tumor simulations starting in the subventricular zone.* **B**, *CPVD and EVD plotted against T1Gd volume for tumor simulations starting in the white matter.*

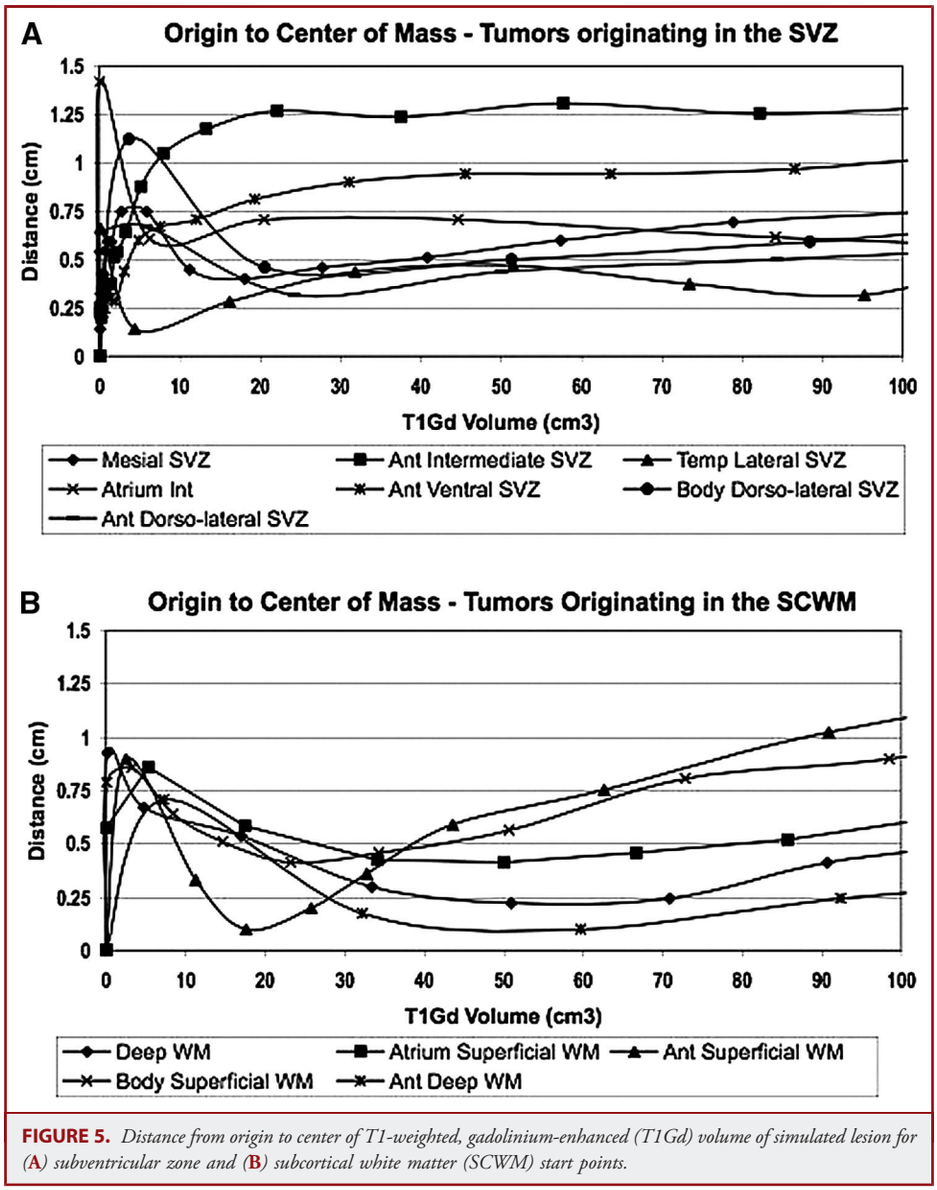

FIGURE 5. *Distance from origin to center of T1-weighted, gadolinium-enhanced (T1Gd) volume of simulated lesion for (A) subventricular zone and (B) subcortical white matter (SCWM) start points.*

P = .007). The difference in size was also striking, although nonsignificant, with a mean volume at simultaneous ventricle and skull contact of 25 cm^3 for SCWM start points compared with 100 cm^3 for SVZ start points (P = .07).

DISCUSSION

This study provides a combination of clinical observations and mathematical modeling to validate the hypothesis that GBMs may arise from cells located in the SCWM and not necessarily from the SVZ. More than half of the GBMs studied were radiographically distinct from the ventricles, whereas in 20% of the tumors, the nearest contrast-enhancing edge was $>$ 1 cm away from the ventricles. Additionally, increasing tumor volume correlated with decreasing tumor EVD but correlated with increasing tumor CPVD, consistent with predictions that tumors originate distant from the SVZ. Tumors with ventricular contact may reflect a growing mass in a limited intracranial space rather than an indication of periventricular origin. This is validated by the growth pattern observed in the patient whose 2 preoperative MRIs separated by 1 month confirmed dramatic tumor growth. Comparison of these 2 studies demonstrated the same pattern; as

the tumor grew, its edge approached the ventricle while the center point-to-ventricle distance did not significantly change.

In tumors that abut the ventricles, increasing tumor volume correlates with increasing CPVD, consistent with our predicted growth pattern. This is consistent with these tumors originating in either the SVZ or potentially in the SCWM and growing to achieve ventricular contact before detection. Thus, our results support that tumors found distant from the ventricles arise in SCWM away from the SVZ; it is not possible to assert the converse that tumors abutting the ventricles necessarily arise from the SVZ. It is also possible that periventricular and deep white matter GBMs represent biologically distinct entities, and there are some emerging data to support this hypothesis, which this article cannot fully address.

The clinical patterns of tumor growth observed in the analysis of single-point-in-time preoperative images for $>$ 60 GBM patients are consistent with the patterns observed in the computer simulations of glioma growth using a previously validated model based on serial imaging. These patterns appeared consistent for tumors in the temporal, parietal, and frontal lobes. Although significant biological and genetic differences almost certainly exist among this population of tumors, the pattern of growth observed on preoperative imaging and the relationship of these tumors to the ventricles are consistent with the modeled results using fixed values for tumor growth and migration rates. The spatial complexity of the brain anatomy can explain much of the diversity in appearances seen in vivo. Although this does not disprove the hypothesis that differences in ontology and cellular phenotype have significant influence on tumor behavior, it does explain much of the observed variability within a very simple paradigm.

Two recent studies looked at similar data with a different perspective and drew different conclusions. One, by Barami et al[38] looking at T1 and T2 sequences, found that 82% of the contrast-enhancing portion of GBMs in their series (49 patients with World Health Organization grade IV tumors) contacted the ventricles on T1-weighted imaging. They did not find a statistically significant relationship between ventricular contact and tumor size. This analysis was conducted for gliomas of all grades, not only GBMs, and the difference between their observations and ours may be in part because, by including lesional contact with ventricles on T2-weighted imaging, they result with the vast majority of tumors in both their large and small size categories having ventricular contact.

A second study, by Lim et al,[37] examined preoperative MRI scans for patients with newly diagnosed GBM, hoping to learn something about glioma ontogeny and phenotype based on the location of the tumors. In contrast to the results of Barami et al but consistent with our results, that study similarly observed that more than half (52%) of the tumors did not have contrast-enhancing regions abutting the SVZ radiographically on T1-weighted imaging. However, combining radiographic data on SVZ and cortical invasion with clinical data on multifocal recurrence of these tumors after initial therapy, the authors concluded that tumors that contacted the SVZ and invaded the cortex exhibited a more malignant and invasive phenotype and that this likely indicated a stem cell origin, at least for these tumors. Although such an explanation is plausible for their results, we did not analyze similar clinical data in our study.

The study by Lim et al[37] infers phenotypic differences between tumors in different location and uses these inferred differences to explain the variance in their rates and patterns of recurrence. We analyze similar radiographic data, assuming that the tumor cells could have the same intrinsic properties regardless of the site of tumor origin but that local environment would affect cell proliferation and dispersion. Specifically, we proposed that glioma cells migrate faster in white matter than gray matter and that cells would tend to pile up at tissue boundaries such as the ventricular margin or the pial surface. The computer model of glioma growth, which assumes a uniform cellular phenotype, generated results consistent with those observed in our patient population, varying only the anatomic start point of the simulated tumors. Tumors that abut both the cortex and the SVZ are likely to be larger, on average, than those that abut only one or neither of these structures. Our simulations suggest that a tumor that abuts both the cortex and the SVZ more likely originated in the SCWM and not, as Lim et al inferred, in the SVZ. Given the wide radiographically silent dissemination of glioma cells, the recurrence patterns of these tumors may represent their advanced dissemination and size rather than a biologically more malignant phenotype, as Lim et al conclude.

The implications of the radiographic appearance of GBMs on their origins must be interpreted with care. Although the modeling suggests that the center of the contrast-enhancing portion of a clinically evident tumor may not be assumed to be equivalent to the point of origin, it supports the idea that the point of origin is contained within the contrast-enhancing portion of the tumor. There are many unknown and perhaps unknowable factors such as the specific cellular events leading to the malignant phenotype of the glioma cell or cells of origin. Our study is limited both by sample size and by the exclusion of a moderate number of patients over the examined period.

Our results show that many tumors do not appear to arise from the SVZ. If one accepts that these tumors may arise from any point in the white matter, then simple assumptions about glioma growth patterns are able to explain much of the variability observed in the radiographic appearance of these tumors. This is not to deny the possibility of significant differences in cellular phenotypes between tumors of different appearances, but we would assert that such differences are not necessary to explain the varied appearance of these tumors at diagnosis. We hope further work incorporating survival data and cellular analysis will further elucidate regional variability and commonality in glioma behavior.

Disclosure

This work was made possible in part by a Doris Duke Clinical Research Fellowship (Dr Bohman), National Institutes of Health grant RO1 CA 89395 (Dr Bruce), a Mary Gates Research Scholarship (J.L. Moore), and a 21st Century Scientist Award from the McDonnell Foundation (Dr Swanson and R. Rockne).

The authors have no personal financial or institutional interest in any of the drugs, materials, or devices described in this article.

REFERENCES

1. Galli R, Binda E, Orfanelli U, et al. Isolation and characterization of tumorigenic, stem-like neural precursors from human glioblastoma. *Cancer Res*. 2004;64(19):7011-7021.
2. Shih AH, Dai C, Hu X, Rosenblum MK, Koutcher JA, Holland EC. Dose-dependent effects of platelet-derived growth factor-B on glial tumorigenesis. *Cancer Res*. 2004;64(14):4783-4789.
3. Singh SK, Clarke ID, Terasaki M, et al. Identification of a cancer stem cell in human brain tumors. *Cancer Res*. 2003;63(18):5821-5828.
4. Bjerkvig R, Tysnes BB, Aboody KS, Najbauer J, Terzis AJ. Opinion: the origin of the cancer stem cell: current controversies and new insights. *Nat Rev Cancer*. 2005;5(11):899-904.
5. Oliver TG, Wechsler-Reya RJ. Getting at the root and stem of brain tumors. *Neuron*. 2004;42(6):885-888.
6. Gil-Perotin S, Marin-Husstege M, Li J, et al. Loss of p53 induces changes in the behavior of subventricular zone cells: implication for the genesis of glial tumors. *J Neurosci*. 2006;26(4):1107-1116.
7. Jackson EL, Garcia-Verdugo JM, Gil-Perotin S, et al. PDGFR alpha-positive B cells are neural stem cells in the adult SVZ that form glioma-like growths in response to increased PDGF signaling. *Neuron*. 2006;51(2):187-199.
8. Quinones-Hinojosa A, Sanai N, Soriano-Navarro M, et al. Cellular composition and cytoarchitecture of the adult human subventricular zone: a niche of neural stem cells. *J Comp Neurol*. 2006;494(3):415-434.
9. Assanah M, Lochhead R, Ogden A, Bruce J, Goldman J, Canoll P. Glial progenitors in adult white matter are driven to form malignant gliomas by platelet-derived growth factor-expressing retroviruses. *J Neurosci*. 2006;26(25):6781-6790.
10. Colin C, Baeza N, Tong S, et al. In vitro identification and functional characterization of glial precursor cells in human gliomas. *Neuropathol Appl Neurobiol*. 2006;32(2):189-202.
11. Ligon KL, Alberta JA, Kho AT, et al. The oligodendroglial lineage marker OLIG2 is universally expressed in diffuse gliomas. *J Neuropathol Exp Neurol*. 2004;63(5):499-509.
12. Mason JL, Goldman JE. A2B5+ and O4+ cycling progenitors in the adult forebrain white matter respond differentially to PDGF-AA, FGF-2, and IGF-1. *Mol Cell Neurosci*. 2002;20(1):30-42.
13. Roy NS, Wang S, Harrison-Restelli C, et al. Identification, isolation, and promoter-defined separation of mitotic oligodendrocyte progenitor cells from the adult human subcortical white matter. *J Neurosci*. 1999;19(22):9986-9995.
14. Ogden AT, Waziri AE, Lochhead RA, et al. Identification of A2B5+CD133-tumor-initiating cells in adult human gliomas. *Neurosurgery*. 2008;62(2):505-514; discussion 514-515.
15. Masui K, Suzuki SO, Torisu R, Goldman JE, Canoll P, Iwaki T. Glial progenitors in the brainstem give rise to malignant gliomas by platelet-derived growth factor stimulation. *Glia*. 2010;58(9)1050-1065.
16. Alcantara Llaguno S, Chen J, Kwon CH, et al. Malignant astrocytomas originate from neural stem/progenitor cells in a somatic tumor suppressor mouse model. *Cancer Cell*. 2009;15(1):45-56.
17. Wang Y, Yang J, Zheng H, et al. Expression of mutant p53 proteins implicates a lineage relationship between neural stem cells and malignant astrocytic glioma in a murine model. *Cancer Cell*. 2009;15(6):514-526.
18. Jackson EL, Alvarez-Buylla A. Characterization of adult neural stem cells and their relation to brain tumors. *Cells Tissues Organs*. 2008;188(1-2):212-224.
19. Kappadakunnel M, Eskin A, Dong J, et al. Stem cell associated gene expression in glioblastoma multiforme: relationship to survival and the subventricular zone. *J Neurooncol*. 2010;96(3):359-367.
20. Recht L, Jang T, Savarese T, Litofsky NS. Neural stem cells and neuro-oncology: quo vadis? *J Cell Biochem*. 2003;88(1):11-19.
21. Glantz M, Kesari S, Recht L, Fleischhack G, Van Horn A. Understanding the origins of gliomas and developing novel therapies: cerebrospinal fluid and subventricular zone interplay. *Semin Oncol*. 2009;36(4)(Suppl 2):S17-S24.
22. Harpold HL, Alvord EC Jr, Swanson KR. The evolution of mathematical modeling of glioma proliferation and invasion. *J Neuropathol Exp Neurol*. 2007;66(1):1-9.
23. Swanson KR. Mathematical Modeling of the Growth and Control of Tumors [dissertation]. Seattle: University of Washington; 1999.
24. Swanson KR, Alvord EC Jr. The concept of gliomas as a "traveling wave": the application of a mathematical model to high- and low-grade gliomas. *Can J Neurol Sci*. 2002;29(4):395.
25. Swanson KR, Alvord EC Jr. Serial imaging observations and postmortem examination of an untreated glioblastoma: a traveling wave of glioma growth and invasion. *Neuro Oncol*. 2002;4(4):340.
26. Swanson KR, Bridge C, Murray JD, Alvord EC Jr. Virtual and real brain tumors: using mathematical modeling to quantify glioma growth and invasion. *J Neurol Sci*. 2003;216(1):1-10.
27. Mandonnet E, Delattre JY, Tanguy ML, et al. Continuous growth of mean tumor diameter in a subset of grade II gliomas. *Ann Neurol*. 2003;53(4):524-528.
28. Swanson KR, Alvord EC Jr, Murray JD. Quantifying efficacy of chemotherapy of brain tumors with homogeneous and heterogeneous drug delivery. *Acta Biotheor*. 2002;50(4):223-237.
29. Swanson KR, Rostomily RC, Alvord EC Jr. A mathematical modelling tool for predicting survival of individual patients following resection of glioblastoma: a proof of principle. *Br J Cancer*. 2008;98(1):113-119.
30. Rockne R, Alvord EC Jr, Rockhill JK, Swanson KR. A mathematical model for brain tumor response to radiation therapy. *J Math Biol*. 2009;58(4-5):561-578.
31. Wang CH, Rockhill JK, Mrugala M, et al. Prognostic significance of growth kinetics in newly diagnosed glioblastomas revealed by combining serial imaging with a novel biomathematical model. *Cancer Res*. 2009;69(23):9133-9140.
32. Cocosco CA, Kollokian V, Kwan KS, Evans AC. BrainWeb: online interface to a 3D simulated brain database. *Neuroimage*. 1997;5(4):S425.
33. Swanson KR, Alvord EC Jr, Murray JD. A quantitative model for differential motility of gliomas in grey and white matter. *Cell Prolif*. 2000;33(5):317-329.
34. Giese A, Kluwe L, Laube B, Meissner H, Berens ME, Westphal M. Migration of human glioma cells on myelin. *Neurosurgery*. 1996;38(4):755-764.
35. Jbabdi S, Mandonnet E, Duffau H, et al. Simulation of anisotropic growth of low-grade gliomas using diffusion tensor imaging. *Magn Reson Med*. 2005;54(3):616-624.
36. Sanai N, Tramontin AD, Quinones-Hinojosa A, et al. Unique astrocyte ribbon in adult human brain contains neural stem cells but lacks chain migration. *Nature*. 2004;427(6976):740-744.
37. Lim DA, Cha S, Mayo MC, et al. Relationship of glioblastoma multiforme to neural stem cell regions predicts invasive and multifocal tumor phenotype. *Neuro Oncol*. 2007;9(4):424-429.
38. Barami K, Sloan AE, Rojiani A, Schell MJ, Staller A, Brem S. Relationship of gliomas to the ventricular walls. *J Clin Neurosci*. 2009;16(2):195-201.

COMMENTS

Can a careful analysis of magnetic resonance images (MRIs) provide clues to the very origin of gliomas? Neural stem cells and glial progenitor cells are observed throughout the neuraxis but are especially concentrated in the subventricular zone (SVZ) and periventricular white matter, creating a substrate for neoplastic transformation.[1] Neoplastic involvement of the ventricular lining represents a challenge to obtain "total" resections and a site of glioma recurrence and cellular resistance to therapy.

In this well-written article, Bohman et al evaluate the relationship between the MRI characteristics and the presumed origin of glioblastoma. Their conclusion, based on T1-weighted gadolinium contrast-enhancing visualization of the MRI, is that glioblastomas originate throughout the white matter and are not limited to the SVZ. As tumors enlarge, ultimately the edges of all tumors will near the ventricles, simply because of physical proximity to the ventricular surface. The strength of the study is the groundbreaking integration of diagnostic imaging with sophisticated mathematical modeling, which has great potential for personalized medicine and clinical trials by predicting tumor growth and response to therapy.

The work, however, is inconclusive because the investigators confined their analysis to the contrast-enhancing portions of tumor and did not

review the equally important T2/fluid-attenuated inversion recovery (FLAIR) views that shed light on the infiltrative component of the disease. Gliomas consist of angiogenic (visualized by contrast MR) and nonangiogenic cell populations that are not detected by conventional imaging.[2] The authors found that approximately one-half (46%) of the gliomas were contiguous and 59% were within 5 mm of the ventricular lining. We reported similar findings in a series of 100 patients treated at the Moffitt Cancer Center: 52% of the tumors, based on T1-weighted contrast enhancement, showed contact between the tumor surface and the ventricular wall.[3] With the inclusion of T2/FLAIR views, an additional 40% of the tumors showed contact with the ventricular wall.[3] Taken together, > 90% of the gliomas showed involvement of the ventricular wall.

In an era of anti–vascular endothelial growth factor (VEGF), antiangiogenic therapy, it is important to evaluate glioma biology and response to therapy using both contrast enhancement and the FLAIR views. The infiltrative, nonangiogenic disease, visualized on FLAIR, could represent angiogenesis-independent clones that are receiving nutrients by passive diffusion from the cerebrospinal fluid across the ependymal lining. Once these cells migrate to and from the subcortical white matter, they can form hypoxic clusters of cells that stimulate the "angiogenesis switch,"[2] becoming visible on contrast-enhanced MR. In support of this hypothesis, Barami et al[3] observed a dozen examples of where the point of contact to the ventricular wall was seen as a "stalk," representing tracts of cells emanating from the SVZ and migrating into nearby parenchyma. These stalks resemble the intravitreal stalks of malignant cells growing in a nonangiogenic environment that migrated to vascularized tissue and grow rapidly once angiogenesis is triggered.[4] The microenvironment of the choroid plexus and surrounding ependyma contains the angiogenic molecule, VEGF, and its receptors.[5] In our view, there are radiographic and biochemical data to suggest an affinity between the ventricular lining and the ultimate formation of angiogenic tumors in the white matter, and this link should be further explored.

The authors report that extension of the glioma boundary to the ventricular wall is a function of the tumor volume. We found a link between tumor volume and contact with the ventricular wall for metastatic tumors but not for gliomas. Metastases larger than 2.3 cm were located near the ventricular lining.[3] Gliomas of all sizes appeared to contact the ventricular walls; the contact of smaller gliomas with the ventricular lining supports a role of the SVZ early in the origin of gliomas.[3] The complex interaction of the cells derived from the ventricular lining provides an opportunity for novel therapies targeted at the SVZ stem cell populations; cerebrospinal fluid–directed therapy could limit the recurrence of glioblastomas.[6]

Overall, the work, despite its preliminary nature, is important and represents the type of studies required to advance the field. The authors should be encouraged to use integrated mathematical modeling for other types of neuroimaging modalities to discern patterns of glioma genesis, growth, vascularization, invasion, therapeutic response, resistance, and recurrence.

Steven Brem
Surbhi Jain
Tampa, Florida

1. Sanai N, Buylla AA, Berger MS. Neural stem cells and the origin of gliomas. *N Engl J Med*. 2005;353(8):811-822.
2. Frangioni JV. New technologies for human cancer imaging. *J Clin Oncol*. 2008;26(24):4012-4021.
3. Barami K, Sloan AE, Rojiani A, Schell MJ, Staller A, Brem S. Relationship of gliomas to the ventricular walls. *J Clin Neurosci*. 2009;16(2):195-201.
4. Brem S, Brem H, Folkman J, Finkelstein D, Patz A. Prolonged tumor dormancy by prevention of neovascularization in the vitreous. *Cancer Res*. 1976;36(8):2807-2812.
5. Maharaj ASR, Walshe TE, Saint-Geniez M, et al. VEGF and TGF-β are required for the maintenance of the choroid plexus and ependyma. *J Exp Med*. 2008;205(2):491-501.
6. Glantz M, Kesari S, Recht L, Fleischhack G, Van Horn A. Understanding the origins of gliomas and developing novel therapies: cerebrospinal fluid and subventricular zone interplay. *Semin Oncol*. 2009;26(4)(suppl 2):S17-S24.

Since Virchow coined the term "glioma" for tumors arising from the brain substance, the glioblastoma has been recognized as a very important yet poorly understood brain tumor. Tumor classification has been an ongoing debate. In the 1979 World Health Organization Classification of Tumors of the Central Nervous System, glioblastoma was a separate category. Later, it was added to the spectrum of astrocytic tumors. This article focuses on the controversy of glioblastoma ontogeny. The authors use a modeling approach to make a rational argument against SVZ pluripotent or stem cell origin for all glioblastomas.

The authors found that tumors adjacent to the ventricle had a relationship with the ventricle similar to modeled tumor growth from the SVZ region. Likewise, tumor not contacting the ventricle had a relationship with the ventricle similar to modeled tumor growth from lobar white matter locations.

The conclusion drawn from observations of real tumor growth and mathematical modeling of tumor growth from different origin sites is that glioblastomas commonly arise from cells located in the lobar white matter and not from the SVZ, although the possibility that some glioblastomas arise from the SVZ and may have a stem cell origin cannot be excluded.

Warren Boling, MD
Morgantown, West Virginia